JOURNAL OF GEOPHYSICAL RESEARCH, VOL. 104, NO. A9, PAGES 19,765–19,772, SEPTEMBER 1, 1999

# Acceleration of the fast solar wind by the emergence of new magnetic flux

L. A. Fisk, N. A. Schwadron, and T. H. Zurbuchen

Department of Atmospheric, Oceanic, and Space Sciences, University of Michigan, Ann Arbor

**Abstract.** Recent observations have shown that small magnetic loops are continuously emerging within supergranules in the solar photosphere. The subsequent reconnection of this emerging flux with field lines which open into the corona should define the Poynting's vector and mass flux into the corona. These two quantities uniquely determine the final energy flow and speed of the steady, fast solar wind. It is also pointed out that if the consequence of the emergence of new flux and its reconnection is lateral displacements of coronal magnetic field lines, this process should increase the magnetic field energy in the corona in a definable manner. The resulting dissipation of this energy, by work done on the plasma or by Joule heating, defines the spatial distribution for the heating of the corona. A simple model is constructed that yields profiles for the acceleration of the fast solar wind and for coronal temperatures that are reasonable.

## 1. Introduction

Recent observations from SOHO have confirmed that small magnetic loops are continuously emerging within supergranules in the solar photosphere [*Schrijver et al.*, 1997, 1998]. The ends of the loops then migrate independently to the edges of the supergranules, where one side reconnects with magnetic field lines of the opposite polarity. It is the purpose of this paper to point out that this emergence of new magnetic flux can be responsible for and can constrain the heating of the solar corona and the acceleration of the solar wind. We construct an MHD model for the acceleration of the fast solar wind in which the emergence of these loops and their subsequent reconnection are the driving processes which heat the solar corona and accelerate the solar wind. The only parameters of the model are the properties of the emerging loops. The model predicts a fast solar wind which contains a number of features that are consistent with observations in the heliosphere.

Over the years, numerous models have been constructed for the acceleration of the solar wind [e.g., *Parker*, 1958; *Isenberg*, 1991, and references therein; *Marsch*, 1994, and references therein; *Hansteen and Leer*, 1995; *Axford and McKenzie*, 1997; *McKenzie et al.*, 1997]. These models frequently need to assume some form for the spatial deposition of energy or momentum into the corona, which is used to describe the heating and acceleration of the corona from, for example, the interaction with waves. The deposition of energy and momentum then determines such quantities as the mass flux and the temperature, density, and Mach number profiles for the solar wind. It is suggested here that the emergence of new magnetic flux may determine both the Poynting's vector and the mass flux into the corona. These two quantities uniquely determine the final energy flux and speed of the solar wind, independent of the exact mechanism by which energy and momentum are deposited. Moreover, if the consequence of the emergence of new flux is to result in lateral displacements of the coronal magnetic field, this process will tend to result in the buildup of magnetic energy in the corona, which when dissipated by doing work on the plasma or by Joule heating yields reasonable profiles for the solar velocity and the coronal temperature.

We concentrate here on the fast solar wind from the quasi-steady polar coronal holes near solar minimum. This wind is observed to be remarkably steady [e.g., *Phillips et al.*, 1995] and is readily discussed in terms of time-stationary or time-averaged theories. Some of the principles discussed here could apply to the slow solar wind but with the proviso that the acceleration of the slow solar wind needs to be considered a dynamic, time-varying process as has been discussed by *Axford* [1977] and *Fisk et al.* [1999].

We begin by reviewing briefly the properties and processes associated with emerging loops. We point out that the resulting Poynting's vector and mass flux into the corona determines the final energy flux and flow speed of the solar wind, regardless of the mechanism by which energy is dissipated and the corona is heated. We then construct a simple model for the acceleration of the solar wind based on these principles, derive the appropriate Mach number equation, and calculate the resulting mean speed and temperature profiles. Concluding remarks are provided in section 5.

## 2. Emergence of New Magnetic Flux in the Photosphere

The magnetic field in the photosphere is highly structured and dynamic down to the resolution limit of modern magnetic field instruments such as the Michelson Doppler Imager on SOHO [*Scherrer et al.*, 1995]. For a review of earlier data, including ground-based observations, refer to *Stenflo et al.* [1998] and *Martin* [1990]. In general, these observations show the following major features.



Paper number 1999JA900256.
0148-0227/99/1999JA900256$09.00

The most readily observable component of the solar magnetic field is the high field concentrations, with field strength of the order of a kilogauss, associated with the edges of supergranules. As described by *Schrijver et al.* [1997, 1998], however, small magnetic bipolar flux elements emerge continuously at random locations within the supergranules. The two elements of this bipolar flux initially separate fairly quickly but then move under the influence of the supergranule flow pattern, with each element often moving independently. The supergranule flow is responsible for the concentration of the flux at the boundaries of the supergranules and typically has a speed of ~400 m $s^{-1}$. The convected bipolar elements then interact with the preexisting flux concentrations. In the case of opposite field polarity, reconnection should occur; in the case of like polarity, the bipolar element enhances the field concentration. This process leads to a continuous evolution of the locations of the field concentrations, with a characteristic time of 1.5 days.

The likely behavior of the bipolar elements is illustrated schematically in Figure 1. In Figure 1a, a small bipolar loop emerges in the center of the supergranule. The edges of the supergranule are marked by field concentrations which include field lines which open into the corona. In Figure 1b, one side of the loop has migrated to a field concentration at the

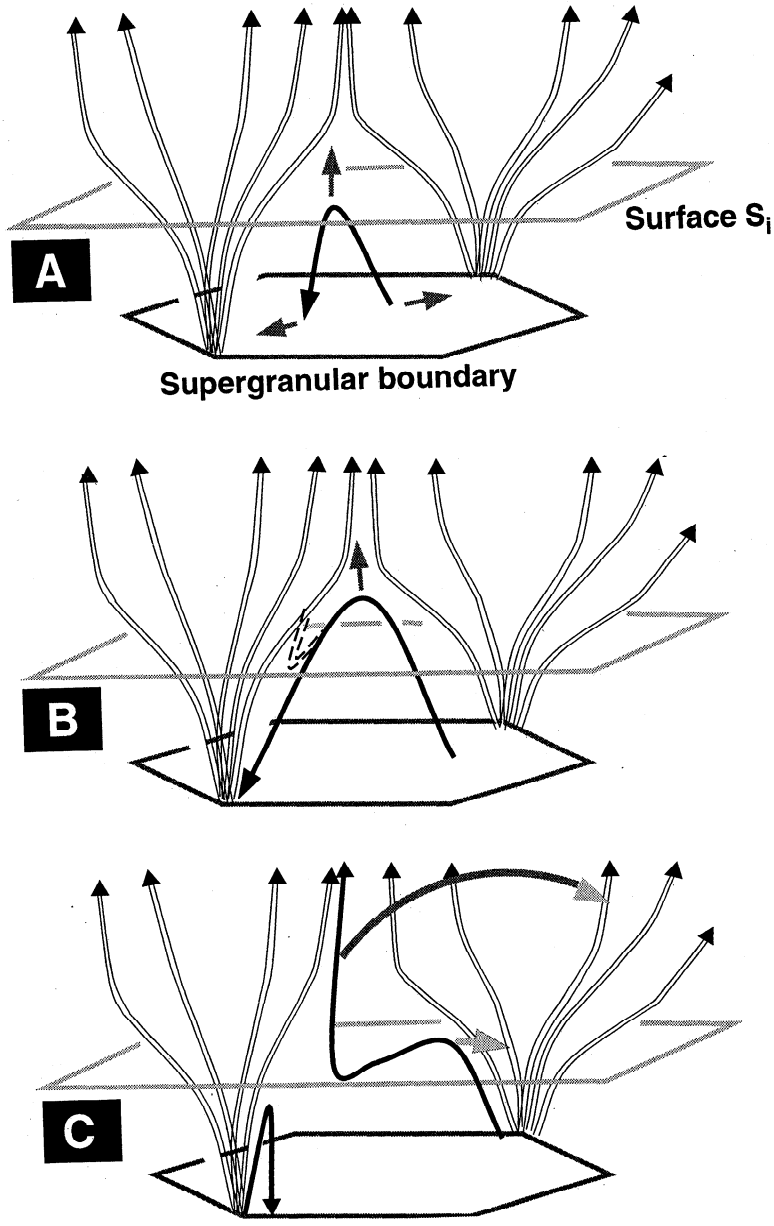


**Figure 1.** An illustration of the expected behavior of emerging magnetic loops in the photosphere. (a) A new loop (shown as solid arrow) emerges in the center of a supergranule. (b) The ends of the loop migrate to the boundaries of the supergranule where there are concentrations of magnetic flux (shown as open lines); only field lines which open into the corona are shown. The end of the loop with polarity opposite to that of the flux concentration reconnects with a field line which opens into the corona. (c) The new open field line is transported laterally to be reoriented over the other side of the loop.

supergranule boundary. The field polarity in this case is opposite, and reconnection presumably occurs. As is shown in Figure 1c, the field line then presumably reorients to be located over the opposite side of the loop, which, in turn, may be convected into another field concentration.

Consider a surface located immediately above the photosphere, as shown in Figure 1. The normal to the surface is in the heliocentric radial direction $\mathbf{e}_r$, and the surface is denoted as $S_i$ for inner surface of the corona. The loops emerge through $S_i$. There is then a Poynting's vector through the surface because of the upward motion of the magnetic field. Assume that the reconnection with a field line which opens into the corona occurs near but above the surface. The magnetic flux in the original loop therefore does not return through the surface, or, equivalently, there is a time-averaged Poynting's vector into the corona because of the emergence of new loops which reconnect with open field lines. We assume that the conductivity of the plasma is infinite and that the electric field is given by $\mathbf{E} = -\mathbf{u} \times \mathbf{B}/c$. The surface integral of this time-averaged Poynting's vector is then given by

$$\int_{S_i} \left\langle \frac{c}{4\pi} \mathbf{E} \times \mathbf{B} \right\rangle \bullet d\mathbf{s} = \int_{S_i} \left\langle \frac{B^2}{4\pi} \mathbf{u}_\perp \right\rangle \bullet d\mathbf{s} = \frac{\overline{B}_l^2 u_l A_i}{4\pi}. \quad (1)$$

Here $\mathbf{E}$ and $\mathbf{B}$ are the electric and magnetic field, respectively, and $c$ is the speed of light; angle brackets denote time average. The velocity of the motion of the loops perpendicular to $\mathbf{B}$ is $\mathbf{u}_\perp$. The magnetic field strength in the emerging loops averaged over the total area $A_i$ of surface $S_i$ and time is $\overline{B}_l$; the upward speed of the loop in the heliocentric radial direction $\mathbf{e}_r$ is $u_l$.

The emerging loops depicted in Figure 1 are the ones that reconfigure the network of flux concentrations. The ends of the loops move independently toward different flux concentrations, and one side of the loop reconnects with a field line which opens into the corona. These emerging loops, then, enhance some flux concentrations and diminish or destroy others. Equivalently, the Poynting's vector associated with these emerging loops can be determined by the rate at which the network and the overlying coronal magnetic field is reconfigured.

We define a timescale $\tau$, during which the upward emergence of magnetic energy, as given by the Poynting's vector in (1), is equal to the total magnetic energy present in the coronal magnetic field, that is,

$$\tau \equiv \frac{W_B' A_i}{\int_{S_i} \left\langle \frac{c}{4\pi} \mathbf{E} \times \mathbf{B} \right\rangle \bullet d\mathbf{s}} = \frac{4\pi W_B'}{\overline{B}_l^2 u_l}, \quad (2)$$

where

$$W_B' = \frac{1}{A_i} \int_{\text{vol}} \frac{B^2}{8\pi} d(\text{vol}) \quad (3)$$

is the energy density of the coronal magnetic field, per unit surface area of $S_i$. The volume in (3) is defined with the inner side equal to $S_i$; there is assumed to be no Poynting's vector through the other sides of the volume.

According to *Schrijver et al.* [1998], $\tau$ is observed to be ~1.5 days. The emergence of new magnetic flux in small bipolar regions, whose ends move independently and which reconnect with open field lines, is sufficient to reconfigure the network and thus the coronal magnetic field on this timescale. Other quantities in (2) can also be specified from observations. Bipolar regions in the photosphere are observed to move laterally with the speed of the supergranule flow or ~400 m $s^{-1}$. As the ends of the loops spread, the tops of the loops presumably rise with a comparable speed, that is, $u_l \sim 400$ m $s^{-1}$. The quantity $W_B'$ can be determined from observations of the heliospheric magnetic field. At 1 AU, the radial component of the heliospheric magnetic field is observed to be $3.5 \times 10^{-5}$ G [*Balogh et al.*, 1995]. The field strength increases toward the Sun as radius squared. During solar minimum, the fast solar wind originates from polar coronal holes which occupy limited regions, that is, of the order of 15%, of the solar surface. The expansion in the cross section of the fast solar wind is then typically by a factor of the order of 5, since fast solar wind occupies about 75% of the heliosphere. The strength of the coronal magnetic field near the solar surface must thus be ~8 G, and in the corona it must decline faster than radius squared. The calculated value for $W_B'$ is then ~ $5.9 \times 10^{10}$ $G^2 cm^{-1}$.

With these values for $\tau$, $u_l$, and $W_B'$, the required mean field strength for emerging loops is $\overline{B}_l \sim 12$ G. Recall that $\overline{B}_l$ is the field strength only of loops which ultimately reconnect with open field lines, and it is averaged over $A_i$ and time. Also, emerging loops will penetrate only a portion of $A_i$. Nonetheless, the required value of $\overline{B}_l$ is reasonable since the magnetic field strength of emerging loops is observed to be in the range 4–40 G [*Stenflo et al.*, 1998].

There are also other emerging loops which do not contribute to the reconfiguration of the network of flux concentrations. A small loop could be convected intact into a single flux concentration. Reconnection should occur which could excite waves on the open field lines. However, this process does not alter the flux concentration nor reconfigure the network.

There should also be emerging loops which do not reconnect with field lines that open into the corona but rather, at some subsequent time, subduct back into the photosphere. Such loops have an upward Poynting's vector when they emerge upward through $S_i$. However, they should have an approximate equal and opposite Poynting's vector when they subduct downward and they make no net contribution to the time averaged Poynting's vector. We are concerned here only with emerging loops which reconnect with open field lines, which will always result in a net upward Poynting's vector through $S_i$.

It should be noted that following reconnection, a small loop is created in the region of strong field concentration from the original open field line and the side of the emerging loop that reconnects. This small loop could also subduct back into the photosphere or perhaps participate in the formation of polar plumes. In any event, the small loop will occupy only a small portion of the surface area in Figure 1 and make little contribution to the net Poynting's vector. For example, the surface $S_i$ can be placed infinitesimally below the region of reconnection with the result that the small loop has an infinitesimally small penetration through $S_i$.

The Poynting's vector in (1) will result in distortions and compressions of the overlying coronal magnetic field which propagate outward through the corona as Alfvenic disturbances. There can also be other sources of Alfven waves in the corona; for example, the magnetic field in the flux concentrations, not undergoing reconnection, could

experience wave-like motions, whose amplitude grows as the waves propagate into the corona. We will not consider the Poynting's vector due to these latter waves, since the Poynting's vector due to emerging loops which reconnect appears to be sufficient to accelerate the fast solar wind.

There will also be mass associated with emerging loops. It is conceivable that the mass on the loops will fall back to the photosphere following reconnection. However, the emerging loop reconnects with an open field line in a region of strong field concentration, where, presumably for pressure balance, the particle pressure on the open field line must be very small. The resulting pressure gradient along the reconnected field line should force the loop material into the corona. This process should then result in a time-averaged mass flux into the corona of

$$\int_{S_i} \langle \rho \mathbf{u} \rangle \bullet d\mathbf{s} = \overline{\rho}_l u_l A_i . \tag{4}$$

Here $\rho$ is mass density and $\overline{\rho}_l$ is the mass density on emerging loops, which reconnect with open field lines, averaged over $A_i$ and time. The mass flux in (4) can readily account for the observed mass flux in the solar wind. The observed density in the fast solar wind at 1 AU is $n \sim 3$ cm$^{-3}$, with a speed of $u \sim 780$ km s$^{-1}$ [*Phillips et al.*, 1995]. The number density increases as radius squared back to the Sun, and then the cross sectional area decreases by a factor of ~5, since polar coronal holes occupy only a limited region of the solar surface. With $u_l \sim 400$ m s$^{-1}$, the required value of $\overline{\rho}_l$ is ~$2.25 \times 10^{-15}$ gm cm$^{-3}$, corresponding to a number density of $\overline{n}_l \sim 1.35 \times 10^{9}$ cm$^{-3}$. Again, this is the density averaged over the surface area $A_i$ and time. Individual loops will have higher densities since only certain loops will reconnect with open field lines, and only a portion of the surface $A_i$ is penetrated by emerging loops.

## 3. Energy Flux and Final Speed of the Solar Wind

The Poynting's vector and mass flux in (1) and (4) determine the energy flux and the final speed of the solar wind, independent of the mechanisms by which the corona is heated and the solar wind accelerated. Consider a single-fluid, MHD model for the solar corona and the solar wind. This model, then, will include the effects of waves where the plasma behaves like a fluid, for example, Alfven and magnetosonic waves; it will include work done by the flow of the plasma; it will include heating due to the dissipation of currents in regions of finite conductivity, for example, current sheets or regions of reconnection.

The equations for the continuity of mass, momentum, and energy are

$$\frac{\partial \rho}{\partial t} + \nabla \bullet \rho \mathbf{u} = 0 , \tag{5}$$

$$\rho \frac{\partial \mathbf{u}}{\partial t} + \rho (\mathbf{u} \bullet \nabla) \mathbf{u} = -\nabla P + \frac{(\nabla \times \mathbf{B}) \times \mathbf{B}}{4\pi} - \frac{\rho G M_0}{r^2} \mathbf{e}_r , \tag{6}$$

$$\frac{3}{2} \frac{\partial P}{\partial t} + \frac{3}{2} (\mathbf{u} \bullet \nabla) P + \frac{5}{2} P \nabla \bullet \mathbf{u} = \mathbf{j} \bullet \left( \mathbf{E} + \frac{\mathbf{u} \times \mathbf{B}}{c} \right) . \tag{7}$$

As before, $\rho$ is the solar wind mass density and $\mathbf{u}$ is the mean flow speed. We take the pressure $P$ to be isotropic and ignore heat flux. The gravitational constant is $G$; the mass of the Sun is $M_0$; $r$ is heliocentric radial distance; $\mathbf{e}_r$ is a unit vector in the heliocentric radial direction; and $c$ is the speed of light. The magnetic field $\mathbf{B}$, the electric field $\mathbf{E}$, and the current density $\mathbf{j}$ are governed by Maxwell's equations, and we will need Ampere's law

$$\nabla \times \mathbf{B} = \frac{4\pi}{c} \mathbf{j} , \tag{8}$$

where we have made the usual MHD assumption and have ignored the displacement current. We take the current density to be given by

$$\mathbf{j} = \sigma \left( \mathbf{E} + \frac{\mathbf{u} \times \mathbf{B}}{c} \right) , \tag{9}$$

where $\sigma$ the conductivity is a scalar which we anticipate is finite only in regions of current sheets or where reconnection occurs.

Equations (8) and (9) can readily be manipulated into a single equation for the magnetic field energy:

$$\frac{\partial \left( B^2 / 8\pi \right)}{\partial t} + \nabla \bullet \left( \frac{c}{4\pi} \mathbf{E} \times \mathbf{B} \right) = -\frac{j^2}{\sigma} - \frac{\mathbf{u}}{4\pi} \bullet (\nabla \times \mathbf{B}) \times \mathbf{B} . \tag{10}$$

As expected, the time change in the magnetic field energy plus the divergence of the Poynting's vector is equal to minus the Joule heating, minus the work done by the magnetic field on the plasma.

Equation (10) can be combined with (5), (6), (7), and (9) to yield a single energy flux equation for the flow:

$$\nabla \bullet \left[ \rho \mathbf{u} \left( \frac{u^2}{2} + \frac{5}{2} \frac{P}{\rho} - \frac{G M_0}{r} \right) + \frac{c}{4\pi} (\mathbf{E} \times \mathbf{B}) \right]$$

$$= -\frac{\partial \left( B^2 / 8\pi \right)}{\partial t} - \frac{3}{2} \frac{\partial P}{\partial t} + \frac{G M_0}{r} \frac{\partial \rho}{\partial t} - \frac{\partial \left( \rho u^2 / 2 \right)}{\partial t} . \tag{11}$$

Consider the average behavior of the solar wind. The magnetic field energy, the plasma pressure, the density, and the kinetic energy of the flow are not, on average, varying with time, or

$$\nabla \bullet \left[ \left\langle \rho \mathbf{u} \left( \frac{u^2}{2} + \frac{5}{2} \frac{P}{\rho} - \frac{G M_0}{r} \right) + \frac{c}{4\pi} (\mathbf{E} \times \mathbf{B}) \right\rangle \right] = 0 , \tag{12}$$

where angle brackets denote time average. We can then integrate (12) over the volume of the solar corona and derive that

$$\int_S \left\langle \rho \mathbf{u} \left( \frac{u^2}{2} + \frac{5}{2} \frac{P}{\rho} - \frac{G M_0}{r} \right) + \frac{c}{4\pi} (\mathbf{E} \times \mathbf{B}) \right\rangle \bullet d\mathbf{s} = 0 , \tag{13}$$

where $S$ defines a closed surface which surrounds the solar corona.

We consider that a solar wind is formed, in which case on an outer surface $S_o$, which can be placed at an arbitrarily large heliocentric distance, $u$ is supersonic and super-Alfvenic, and the Poynting's vector is unimportant. We take the inner surface $S_i$ to be the same as in Figure 1 and (1) and (4), and to lie directly above the photosphere, where it is penetrated by emerging loops. Here the square of the mean flow speed and the sound speed ($5P/3\rho$) will be small relative to $GM_0/r$. We

close the surface with sides that lie parallel to **u** and assume no Poynting's vector through these side surfaces, in which case

$$\int_{S_i}\left\langle\frac{c}{4\pi}(\mathbf{E}\times\mathbf{B})\right\rangle\bullet d\mathbf{s}-\frac{GM_0}{r_i}\int_{S_i}\langle\rho\mathbf{u}\rangle\bullet d\mathbf{s}=\int_{S_o}\left\langle\rho\mathbf{u}\frac{u^2}{2}\right\rangle\bullet d\mathbf{s}, \quad (14)$$

where $r_i$ is the heliocentric radius of the inner surface, that is, 1 solar radius. The final energy flux of the fast solar wind is thus determined entirely by the Poynting's vector and mass flux introduced by emerging loops that reconnect with open field lines, (1) and (4).

From (5),

$$\int_{S_i}\langle\rho\mathbf{u}\rangle\bullet d\mathbf{s}=\int_{S_o}\langle\rho\mathbf{u}\rangle\bullet d\mathbf{s}. \quad (15)$$

Thus, if we take the flow speed to be uniform across the outer surface, the final flow speed of the solar wind $u_f$ is given simply by

$$\frac{u_f^2}{2}=\frac{\int_{S_i}\left\langle\frac{c}{4\pi}(\mathbf{E}\times\mathbf{B})\right\rangle\bullet d\mathbf{s}}{\int_{S_i}\langle\rho\mathbf{u}\rangle\bullet d\mathbf{s}}-\frac{GM_0}{r_i}. \quad (16)$$

From (1) and (4), the final speed of the fast solar wind thus depends only on the properties of emerging loops that reconnect with open field lines as

$$\frac{u_f^2}{2}=\frac{\overline{B}_l^2}{4\pi\overline{\rho}_l}-\frac{GM_0}{r_i} \quad (17)$$

or, by using the definitions of $\tau$ and $W_B'$ in (2) and (3), as

$$\frac{u_f^2}{2}=\frac{W_B'}{\overline{\rho}_l u_l\tau}-\frac{GM_0}{r_i}. \quad (18)$$

Each of the parameters on the right side of (18), $W_B'$, $\overline{\rho}_l u_l$, and $\tau$, can be determined from observations. As described in section 2, the observed magnetic field in the heliosphere yields $W_B'\sim5.9\text{x}10^{10}$ G$^2$cm. The mass flux observed in the heliosphere yields $\overline{\rho}_l u_l$ or, again from section 2, with $u_l\sim400$ m s$^{-1}$ for the upward speed of the loops, $\overline{\rho}_l \sim 2.25\text{x}10^{-15}$ gm cm$^{-3}$. The characteristic time for the introduction of new magnetic energy into the corona is observed to be $\tau \sim 1.5$ days [*Schrijver et al.*, 1998]. With these values in (18), the final speed of the fast solar wind is found to be 780 km s$^{-1}$, as observed [*Phillips et al.*, 1995].

It should be noted that in (17) the final speed of the solar wind depends only on the properties of emerging loops that reconnect with open filed lines $\overline{B}_l$ and $\overline{\rho}_l$. Thus the final speed is independent of the expansion of the solar wind through the corona, that is, the extent to which the solar wind from the polar coronal hole undergoes a nonradial expansion. To the extent, then, that the emergence of new loops is uniform across the photosphere underlying the polar coronal hole, we should expect that the final speed of the fast solar wind is similarly uniform in heliocentric latitude and longitude, as observed [*Phillips et al.*, 1995]. To be sure the mass flux of the solar wind does depend on the cross-sectional area (equation (4)) and thus on the expansion and could vary with latitude and longitude. However, the magnetic field strength in the high corona is expected to be of uniform strength [*Balogh et al.*, 1995], and thus to the extent that the average magnetic field strength of open field lines in the photosphere is similarly uniform, the expansion of the cross-sectional area will not be a function of latitude and longitude, and uniform mass flux will result, again as is observed [*Phillips et al.*, 1995].

## 4. Actual Heating of the Solar Corona and the Resulting Mean Speed and Temperature Profiles

The calculation to this point is quite general. It does not require that the heating or acceleration mechanism for the solar wind be specified; it requires only that a solar wind be formed. Consider, however, the case illustrated in Figure 1c. The continuous reorganization of the base of the coronal magnetic field causes lateral displacements of the coronal field lines through the emergence of new loops and their reconnection. This process will tend to increase the magnetic flux in some regions to $\mathbf{B}_o+\delta\mathbf{B}$ and to decrease it in other regions to $\mathbf{B}_o-\delta\mathbf{B}$. There is no net change in the total magnetic flux by this process; however, the magnetic energy density of the corona increases by $\delta B^2/8\pi$. Said another way, the emergence of new loops and their subsequent reconnection with open field lines will inherently introduce magnitude variations in the magnetic field at the base of the corona, which will propagate into and introduce magnitude variations at higher altitudes. These magnitude variations in the magnetic field cannot be sustained since they will result in magnetic pressure gradients or perhaps in more complicated field configurations with current sheets. The consequence of these magnitude variations, with their increase in magnetic energy density, will thus be to do work on the solar wind plasma and perhaps to Joule heat thereby heating the solar corona and accelerating the solar wind.

Random lateral displacements of the magnetic field lines should increase the magnetic energy density in a volume of the corona in proportion to the magnetic energy density of the volume. The process is simply a lateral displacement of existing field lines into regions of increased and decreased flux. For any given volume of the corona then, the injection of magnetic energy due to the displacement of field lines should be governed by

$$\nabla\bullet\left\langle\frac{c}{4\pi}\mathbf{E}\times\mathbf{B}\right\rangle=-\alpha\frac{B^2}{8\pi}, \quad (19)$$

where $\alpha$ is a constant. The sign is negative since a negative divergence results in an increase in field energy density. The assumption of constant $\alpha$ should fail with increasing distance from the Sun, but may be valid where the field is strong, within the Alfven point.

The quantity $\alpha$ can be evaluated by integrating (19) over the volume of the corona or

$$\int_{S_i}\left\langle\frac{c}{4\pi}\mathbf{E}\times\mathbf{B}\right\rangle\bullet d\mathbf{s}=\alpha\int_{\text{vol}}\frac{B^2}{8\pi}d(\text{vol}), \quad (20)$$

where we assume that there is only a Poynting's vector through the inner surface $S_i$; that is, the lateral displacements of the magnetic field will eventually dissipate. From (1), (2), and (3) then,

$$\alpha=\frac{1}{\tau}=\frac{\overline{B}_l^2 u_l}{4\pi W_B'}. \quad (21)$$

Equations (19) and (21) determine the rate at which and the spatial variation over which magnetic energy is deposited in the corona; no further specification of a heating function is required.

For simplicity, consider a steady state model for the acceleration of the solar wind in which the mean magnetic field lies in the heliocentric radial direction $\mathbf{e}_r$. More complicated expansions could be used, that is, an over-radial expansion such as defined by *Kopp and Holzer* [1976], but it should not alter the basic conclusions. Conservation of mass flux thus requires that

$$\rho u r^2 = \overline{\rho}_l u_l r_i^2, \tag{22}$$

where again $\overline{\rho}_l$ denotes the mean density of the emerging loops, averaged over $A_i$ and time, or as in section 2, $\overline{\rho}_l$ ~$2.25\times10^{-15}$ gm cm$^{-3}$ and $u_l$ ~ 400 m s$^{-1}$.

Equations (21) and (19) can be combined with (12) to yield

$$\frac{1}{r^2}\frac{d}{dr}\left[r^2\rho u\left(\frac{u^2}{2}+\frac{5}{2}\frac{P}{\rho}-\frac{GM_0}{r}\right)\right]=\frac{\overline{B}_l^2 u_l}{4\pi r_i}\left(\frac{r_i}{r}\right)^4, \tag{23}$$

where again $\overline{B}_l$ is the mean magnetic field of the emerging loops that reconnect with open field lines, averaged over $A_i$ and time, or as in section 2, $\overline{B}_l$ ~ 12 G. We are ignoring here the random velocities associated with the lateral motions of the field lines, which could enter into the $u^2$ term. We assume that these motions are small compared to the thermal speed and $\overline{B}_l^2/4\pi\overline{\rho}_l$ and that the dissipation of magnetic energy into heat is rapid.

With (22), we can solve (23) to yield a constant of the motion of the flow

$$A=\frac{u^2}{2}+\frac{5}{2}\frac{P}{\rho}-\frac{GM_0}{r}+\frac{\overline{B}_l^2}{4\pi\overline{\rho}_l}\left(\frac{r_i}{r}\right). \tag{24}$$

The remaining solar wind equation is conservation of momentum, (6), which we take as

$$\rho u\frac{du}{dr}=-\frac{dP}{dr}-\frac{GM_0\rho}{r^2}. \tag{25}$$

We have assumed here that the magnetic field variations are radial, the result of lateral displacements in the field, and thus the magnetic field exerts no direct force on the mean flow. We are thus ignoring the wave pressure of the Alfvenic fluctuations which set up the magnitude variations. This assumption is valid, as is the case here, when the resulting particle pressure $P$ is large compared with any likely wave pressure.

Equations (22), (24), and (25) can be combined into the usual Mach number equation ( $M^2=u^2/(5P/3\rho)$ ) or

$$\left(M^2-1\right)\frac{1}{M}\frac{dM}{dr}=\frac{\left(1+M^2/3\right)}{2\left(A+\frac{GM_0}{r}-\frac{\overline{B}_l^2 r_i}{4\pi\overline{\rho}_l r}\right)}\left[\frac{4A}{r}-5\left(1+\frac{M^2}{3}\right)\frac{\overline{B}_l^2}{4\pi\overline{\rho}_l}\left(\frac{r_i}{r^2}\right)\right]. \tag{26}$$

There is a critical point, $M$=1, at

$$r_c=\frac{5}{3}\frac{\overline{B}_l^2 r_i}{4\pi\overline{\rho}_l A}. \tag{27}$$

Or since from (17), $A=\overline{B}_l^2/4\pi\overline{\rho}_l-GM_0/r_i$,

$$r_c=(5/3)r_i/\left[1-\frac{GM_0}{r_i}\left(\frac{4\pi\overline{\rho}_l}{\overline{B}_l^2}\right)\right]. \tag{28}$$

Again, the location of the critical point and the Mach number profile which results from (26) depend only on the parameters of the emerging loops, which, in turn, define the Poynting's vector and mass flux into the corona. With the values $\overline{\rho}_l$ ~ $2.25\times10^{-15}$ gm cm$^{-3}$ and $\overline{B}_l$ ~ 12 G, the critical point is at 2.75 solar radii, which is reasonable.

Equation (26) can readily be solved numerically with the solution chosen to pass through the critical point given in (28). The resulting solution for $M(r)$ can then be used to calculate the temperature $T(r)$ and flow speed $u(r)$. The sound speed or, equivalently, the temperature is determined from (24) or

$$c_s^2=\frac{10}{3}\frac{kT}{m_p}=\frac{A+GM_0/r-\left(\overline{B}_l^2/4\pi\overline{\rho}_l\right)\left(r_i/r\right)}{\frac{1}{2}\left(M^2+3\right)}, \tag{29}$$

where we have taken the proton and electron temperatures to be equal; $k$ is the Boltzmann equation and $m_p$ is the mass of a proton. The flow speed is then $u=Mc_s$.

The resulting profiles for $T$ and $u$ are shown in Figure 2, with $\overline{\rho}_l$ ~ $2.25\times10^{-15}$ gm cm$^{-3}$ and $\overline{B}_l$ ~ 12 G. The acceleration of the solar wind in this model is quite rapid and consistent with the inferred speed profile of, for example, *Habbal et al.* [1995]. The temperature peaks at ~ $3.8\times10^6$ K, just before the critical point. Again, we have taken the proton and electron temperatures to be equal. In fact, the electron temperature in the corona is expected to be smaller than the proton temperature, for example, the charge composition of the solar wind is determined by an electron temperature less than $2\times10^6$ K [e.g., *Ko et al.*, 1997]. The proton temperature required to yield the sound speed in (29) must thus be ~$5.5\times10^6$ K. Such large proton temperatures are characteristic of models for the acceleration of the fast solar wind which are driven by thermal pressure [e.g., *McKenzie et al.*, 1997].

It should also be noted that the decrease in temperature beyond the critical point in Figure 2 should be adjustable. In the model here, heating is assumed to be continuous, that is, $\alpha$ in (19) is constant. In practice, the lateral displacements of the field lines should diminish with $r$, and the plasma should eventually cool adiabatically. If this transition occurs at sufficiently large $r$, there should be only a minor effect on the final speed of the solar wind but a more significant effect on the plasma temperature in the heliosphere.

Finally, we note that the solution for the temperature in (29) requires that the constant $A$ be specified, which through (24) requires that the temperature be known at one location, for example, at the inner boundary $r=r_i$. In the solution plotted in Figure 2, $A=\overline{B}_l^2/4\pi\overline{\rho}_l-GM_0/r_i$, or, equivalently, the temperature at $r=r_i$ is taken to be zero. The solution for the temperature plotted in Figure 2 thus cannot be used to determine the temperature at $r=r_i$. It is valid, however, elsewhere in the corona since the temperature at the inner boundary is expected to be small and makes at most a very small correction to $A$. For example, if the temperature is less than 100,000 K, the correction to $A$ is less than 0.005. To find the temperature at the inner boundary, it would be necessary to perform an iterative process; a temperature at the inner boundary is assumed; a Mach number solution which passes through the critical point is established; a temperature

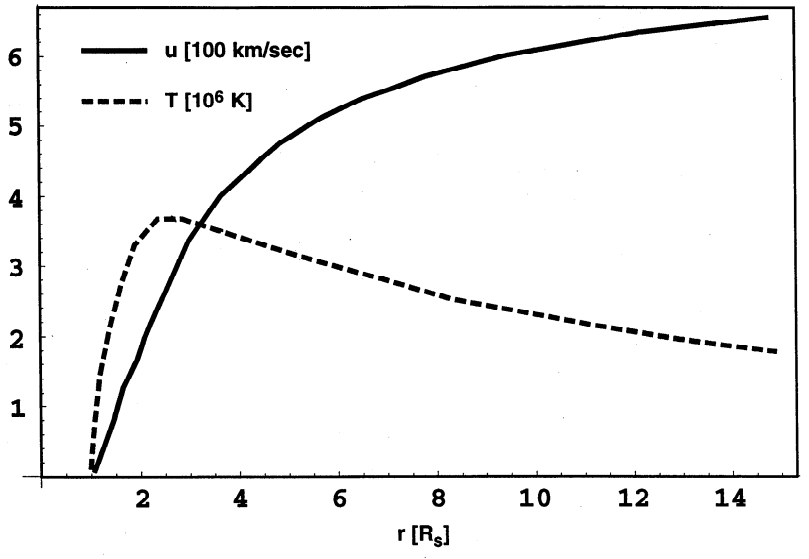


**Figure 2.** The solar wind flow speed $u$ and temperature $T$ as a function of heliocentric radius, as determined by equations (26) and (29), with the parameters described in the text.

profile is determined; and the consistency of the temperature at the inner boundary is checked.

As in any solar wind model, the solution to (26) must have an initial Mach number at the inner boundary $r=r_i$, such that the solution will pass through the critical point at $r=r_c$. In this model, the mass flux is specified, and to the extent that we can specify the initial density separately, we are thus fixing the initial speed. The variable, then, that must be adjusted so that the solution passes through the critical point is the initial sound speed or, equivalently, the initial temperature and pressure. The corona is heated by the deposition of magnetic energy, and to obtain the required critical solution and thus achieve the proper boundary conditions at infinity, the temperature at $r=r_i$ must adjust.

## 5. Concluding Remarks

We have pointed out that the emergence of new magnetic flux in the photosphere and its subsequent reconnection with open magnetic field lines may define the Poynting's vector and the mass flux into the corona. These two quantities uniquely determine the final energy flux and speed of the steady, fast solar wind. Clearly, there is an opportunity here for observational tests. More detailed and statistical observations of the properties of emerging loops can be compared with the final flow properties of the fast solar wind.

We have also pointed out that if the consequence of the emergence of new flux and its reconnection is lateral displacements of coronal magnetic field lines, this process should increase the magnetic field energy in the corona in a definable manner. The resulting dissipation of this energy, by work done on the plasma or by Joule heating, defines the spatial distribution for the heating of the corona. A simple model has been constructed which yields profiles for the acceleration of the solar wind and for coronal temperatures that are reasonable.

The models used here are simple one fluid MHD models, with isotropic pressure and no heat flux. Dissipation by resonant interactions is not included, nor are anisotropic pressure distributions. Clearly, it will be important to test the conclusions drawn here on more detailed models. However, it may turn out that the fundamental issue for the acceleration of the steady, fast solar wind is not the details of how the energy is dissipated in the corona, but rather how emerging loops at the base of the corona inject magnetic energy and mass.

**Acknowledgments.** We thank C. J. Schrijver for very useful discussions on the SOHO observations of emerging magnetic flux. This work was supported, in part, by NASA contracts NAG5-2810 and NAG5-7111 and JPL contract 955460. N.A.S. and T.H.Z. were also supported, in part, by NASA grant NAG5-6471 and NSF grant ATM 9714070.

Janet G. Luhmann thanks Steven T. Suess and another referee for their assistance in evaluating this paper.

## References

Axford, W. I., The three-dimensional structure of the interplanetary medium, in *Study of Traveling Interplanetary Phenomena*, edited by M. A. Shea, D. F. Smart, and S.-T. Wu, p. 145, D. Reidel, Norwell, Mass., 1977.

Axford, W. I., and J. F. McKenzie, The solar wind, in *Cosmic Winds in the Heliosphere*, edited by J. R. Jokipii, C. P. Sonett, and M. S. Giampapa, p. 31, Univ. of Ariz. Press, Tucson, 1997.

Balogh, A., E. J. Smith, B. T. Tsurutani, D. J. Southwood, R. J. Forsyth, and T. S. Horbury, The heliospheric magnetic field over the south polar region of the Sun, *Science*, *268*, 1007, 1995.

Fisk, L. A., T. H. Zurbuchen, and N. A. Schwadron, On the coronal magnetic field: Consequences of large-scale motions, *Astrophys. J.*, in press, 1999.

Habbal, S. R., R. Esser, M. Guhathakurta, and R. R. Fisher, Flow properties of the solar wind from a two-fluid model with constraints from white light and in situ interplanetary observations, *Geophys. Res. Lett.*, *22*, 1465, 1995.

Hansteen, V. H., and E. Leer, Coronal heating, densities and temperatures and solar wind acceleration, *J. Geophys. Res.*, *100*, 21,577, 1995.

Isenberg, P. A., The solar wind, in *Geomagnetism*, vol. 4, edited by J. A. Jacobs, p. 1, Academic, San Diego, Calif., 1991.

Ko, Y.-K., L. A. Fisk, G. Gloeckler, and M. Guhathakurta, An empirical study of the electron temperature and heavy ion velocities in the south polar coronal hole, *Sol. Phys.*, *171*, 345, 1997.

Kopp, R. A., and T. E. Holzer, Dynamics of coronal hole regions, 1, Steady polytropic flows with multiple critical points, *Sol. Phys.*, *49*, 43, 1976.

Marsch, E., Theoretical models for the solar wind, *Adv. Space Res.*, *14*, No. 4, 103, 1994.

Martin, S. F., Small-scale magnetic features observed in the photosphere, in *Solar Photosphere: Structure, Convection, and Magnetic Fields*, edited by J. O. Stenflo, p. 129, Kluwer Acad., Norwell, Mass., 1990.

McKenzie, J. F., W. I. Axford, and M. Banaszkiewicz, The fast solar wind, *Geophys. Res. Lett.*, *24*, 2877, 1997.

Parker, E. N., Dynamics of the interplanetary gas and magnetic fields, *Astrophys. J.*, *128*, 664, 1958.

Phillips, J. L., et al., Ulysses solar wind plasma observations at high southerly latitudes, *Science*, *268*, 1030, 1995.

Scherrer, P. H., et al., The solar oscillations investigation - Michelson doppler imager, *Sol. Phys.*, *162*, 129, 1995.

Schrijver, C. J., A. M. Title, A. A. van Ballegooijen, H. J. Hagenaar, and R. A. Shine, Sustaining the quiet photospheric network: The balance of flux emergence, fragmentation, merging, and cancellation, *Astrophys. J.*, *487*, 424, 1997.

Schrijver, C. J., A. M. Title, K. L. Harvey, N. R. Sheeley Jr., Y.-M. Wang, G. H. J. van den Oord, R. A. Shine, T. D. Tarbell, and N. E. Hurlburt, Large-scale coronal heating by small-scale magnetic field at the Sun, *Nature*, *394*, 152, 1998.

Stenflo, J. O., C. U. Keller, and A. Gandorfer, Differential Hanle effect and the spatial variation of turbulent magnetic fields on the Sun, *Astron. Astrophys.*, *329*, 319, 1998.

L.A. Fisk, N.A. Schwadron, T.H. Zurbuchen, University of Michigan, Department of Atmospheric, Oceanic, and Space Sciences, 2455 Hayward Street, Ann Arbor, MI 48109-2143. (lafisk@umich.edu; nathanas@umich.edu; thomasz@umich.edu)

(Received January 4, 1999; revised May 11, 1999; accepted June 7, 1999.)